International Journal of Applied Engineering Research ISSN 0973-4562 Volume 13, Number 8 (2018) pp. 6026-6035

Dielectric Properties of Cr-Substituted Cobalt Ferrite Nanoparticles Synthesis by Citrate-Gel Auto Combustion Method

Ali M. Mohammad*, Sabah M. Ali Ridha and Tahseen H. Mubarak *****

**University of Garmian, College of Education, Department of Physics-Iraq.*

***University of Kirkuk, College of Education for Pure Sciences, Department of Physics-Iraq.*

****University of Diyala, College of Science, Department of Physics-Iraq.*

Abstract

A series of Cr-substituted cobalt ferrite nanoparticles $CoCr_xFe_{2-x}O_4$ with ($0.0 \leq x \leq 1.0$ with an interval of 0.2), have been synthesized using citrate-gel auto combustion method, the as burnt powders calcined at 600, 700, and 800 ˚C for 3h, and the powders that calcined at 800 ˚C were pressed into a disk shape compacts and sintered in air at 900 ˚C for 3h to study the dielectric properties. The structural properties of all prepared samples was carried out by X-ray diffraction (XRD), the results confirm the formation of spinel cubic structure and revealed the secondary phase with increasing Cr^{3+} contents $0.4 \leq x \leq 1.0$ for the sample that calcined at 600 and 700 ˚C, whereas the samples that calcined at 800 ˚C showed formation of spinel cubic structure with single phased for all Cr-substituted. Moreover, the substitution of Cr^{3+} ions caused a significant reduction in crystallite size. The FE-SEM image results show the some agglomerated of spherical and polyhedral shape morphology with fine size in the range of (44-68 nm). The dielectric parameters such as dielectric constant, dielectric loss (angle and factor) and ac conductivity for all samples were studied as a function of frequency at room temperature by using LCR meter. Variation of dielectric properties at frequencies from 50Hz to 1MHz has been explained on the basis of the Koop's theory, Maxwell-Wagner polarization process, and hoping of electrons. All dielectric properties showed a normal behavior with increasing the frequency

Keywords: Nanoparticle ferrites; Spinel ferrites; Citrate-gel auto combustion; X-ray diffraction; FE-SEM; Dielectric properties; Cr-Co ferrites.

INTRODUCTION

In the recent years ferrites nanoparticles and their composites have been extensively studied by many investigators using various methods due to their interesting electric and magnetic properties, which can be utilized in a wide range of technological applications [1-3], including magnetic recording media, wave absorber, microwave devices, and active compounds [4, 5]. The ferrite nanoparticles have a spinel structure and the general formula is AB_2O_4 [6]. Cobalt ferrite $CoFe_2O_4$ is a most versatile and hard magnetic material, which partially inverted spinel structure with cobalt atoms predominantly in the octahedral sites [2, 7]. The magnetic moment of Fe^{3+} ions ($M=5\mu_B$) occupying the tetragonal A-sites, while the other one contains ferromagnetically Co^{2+} ions ($M=3\ \mu_B$) and Fe^{3+} ions occupying the octahedral B-sites of the spinel structure [6]. In spinel ferrites, addition of metal cations of different valence states leads to various tetrahedral (A) and octahedral (B) sites distributions [8]. As many important properties of the spinel ferrites depend on the nature of the cation distribution over the octahedral and tetrahedral sites in the spinel cubic lattice [9, 10], then any change in distribution of cations among tetrahedral and octahedral site have very dominant effects on the physical properties [6]. Chromium substitution in cobalt ferrite could produce sufficient changes in spinal structure, and the substitution of Cr^{3+} ions have strong B-site preference for Fe^{3+} ions will alter magnetic properties [11] and enhancing the electrical resistivity for sensors and actuator applications [12]. Recently viewed, synthesis of ferrites nanoparticle is one of the interesting fields of material science and technology, there are different methods to synthesized ferrites nanoparticle such as microemulsion [13], ceramic [14], co-precipitation [8], hydrothermal [15], and citrate-gel auto combustion method [16]. In the present work, we have employed citrate-gel auto combustion method to synthesize Cr-substituted cobalt ferrite nanoparticles, because of its simplicity, good stoichiometric control, inexpensive precursors, ultrafine particles, short processing time at very low temperature and other properties of the materials [17]. The aim of present work is to study the influence of Cr-substitution on the structural, dielectric properties of cobalt ferrite $CoCr_xFe_{2-x}O_4$ ($0.0 \leq x \leq 1.0$, step 0.2).

EXPERIMENTAL DETAILS

Synthesis

Nanoparticles ferrite with chemical formula $CoCr_xFe_{2-x}O_4$ (x=0.0, 0.2, 0.4, 0.6, 0.8, and 1.0) were synthesized in air using citrate-gel auto combustion method. Stoichiometric amounts of ferric nitrate $Fe(NO_3)_3.9H_2O$, cobalt nitrate $Co(NO_3)_2.6H_2O$, chromium nitrate $Cr(NO_3)_3.9H2O$ and citric acid $C_6H_8O_7$ in mole ratio of 1:1 were weighed and dissolved separately in minimum amount of deionized water to form a mixed solution. After stirring the solutions were mixed and pH of the resulting solution was adjusted to 7 by adding ammonia solution dropwise [18]. The obtained solutions were transformed into a viscous gel phase by slowly increasing the temperature of hot plate to 90 °C for 2 h under continuous

stirring. During evaporation, the solution became a very viscous brown gel. When finally all water molecules were removed from the mixture, the viscous gel was placed on an oven and heated at 275-300 ℃ to initiate an auto combustion reaction and produce as-burnt ferrite powder. The as burnt powder after combustion was calcined at 600, 700, and 800 ˚C for 3h to remove organic waste and to improve the homogeneity, where the samples that calcined at 800 ˚C added with a small amount 2% PVA as a binder to press it into circular pellets of diameter 12 mm with thickness about 2 mm by applying a pressure of 3 tons using a hydraulic press, then the prepared pellets were sintered at 900 ℃ for 3h for the densification of the sample and slowly allowed to cool naturally for investigations the dielectric properties.

Characterizations

The crystal structure of the synthesized samples were characterized using X-Ray Diffraction (XRD), model PANalytical (X'pert Pro, Netherlands) equipped with high-intensity Cu kα radiation source (λ= 0.154 nm, 40 mA, 40 kV) in the 2θ range 15°- 80°. Surface morphology were carried out by Field Emission Scanning Electron Microscopy (FE-SEM), using (FE-SEM; Model Mira3-XMU, TESCAN, japan). The dielectric measurements were made by using a home-made cell and LCR meter type (LCR-8105G) manufactured by GW INSTEK at room temperature in the frequency range 50Hz to 1MHz.

RESULTS AND DISCUSSION

Structural properties

The XRD patterns of Cr-substituted cobalt ferrite $CoCr_xFe_{2-x}O_4$ (x=0.0, 0.2, 0.4, 0.6, 0.8, and 1.0) for as-burnt and the calcined powders at different temperature 600, 700 and 800℃ are shown in Fig. 1(a-f). The absence of spinal ferrite peak in the XRD of the as-burnt indicates the amorphous nature of the samples. However, the calcined samples at 600 and 700 ˚C confirm the formation of spinel cubic structure and an additional peaks have been observed and designated by symbol * which may be due to the presence of potassium cobalt sulfite $K_2Co_2(SO_4)_3$, which represents a secondary phase appeared, with exceeding the limit of Cr-substitution after x= 0.4. The calcined powder samples at 800 ˚C showed the formation of spinel cubic structure with single phased for all Cr-substituted. The broad peaks at 600℃ signify lower crystallite size of the synthesized sample and as the calcined temperature is increased, the peaks become sharp due to increase in the grain size.

The XRD pattern shows that all reflection peaks of the powders that calcined at 600, 700, and 800℃ corresponding to (220), (311), (222), (400), (422), (511) and (440) planes in pure (x=0) and different Cr-substituted cobalt ferrites. The peak position in XRD patterns are perfectly matched the standard pattern with reference code ICSD 00-001-1121 for pure $CoFe_2O_4$ and 01-076-2496 for Cr-substituted $CoFe_2O_4$.

Our results show that the crystallite size was found to increase with calcined temperature and this can be attributed to the grain growth of the particles, as increases in the calcination temperature, the diffraction peaks become sharper and narrower, and their intensity increases[19]. This indicates intensification in crystallinity that originates from the increment of crystalline volume ratio due to the particle size enlargement of the nuclei [20], which is well agreed with the earlier report[21].

The crystallite sizes (D) of each sample was estimated from Scherrers formula and taking the highest intensity peak (311) for consideration, the lattice constant (a), density (ρ_x) and the hopping length in A-site (L_A) tetrahedral and B-site (L_B) octahedral were calculated from the relations given below [22].

$$D = \frac{0.96\lambda}{\beta.\cos\theta} \quad (1)$$

$$a = d_{hkl}\sqrt{h^2 + k^2 + l^2} \quad (2)$$

$$\rho_x = \frac{8M}{Na^3} \quad (3)$$

$$L_A = 0.25a\sqrt{3} \quad (4)$$

$$L_B = 0.25a\sqrt{2} \quad (5)$$

Where λ is the wavelength of X-ray, β is the full width at half maximum of the concerned peak, d is spacing between the planes, (h, k, l) are the miller indices, M is molecular weight of the composition, and N is avogadro number.

Data in Table 1 is calculated from the above relations. It is observed the value of crystallite size (D) goes on decreasing with increase in Cr-substitution. The same trend in variation of crystallite size was observed in Cr-substituted magnesium ferrospinels and Al substituted nickel ferrites [23, 24].The crystallite size is found as 49.638, 54.161, and 59.149 nm for the samples that calcined at 600, 700 and 800℃ respectively for pure (x = 0.0), while the crystallite size decreases with increasing Cr^{3+} ions, as the substituent ions inhibiting the grain growth. Table 1 clearly shows an increase in the calcined temperature the grain size has been increased which may be attributed to that the specific surface area of the particle decreases with the increase in calcined temperature, which are very much agreed with the earlier reports [25].

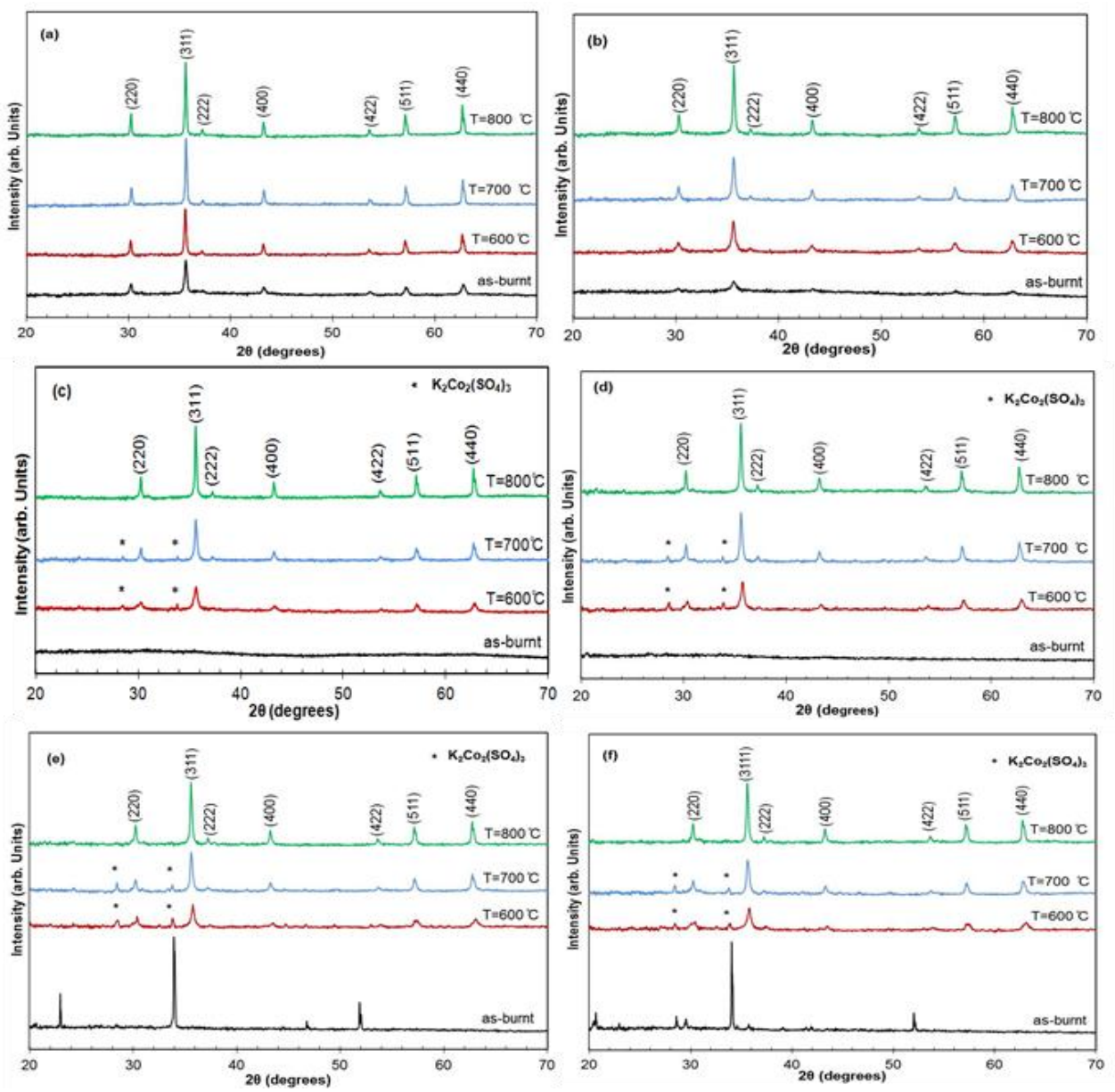

Figure 1. XRD patterns of $CoCr_xFe_{2-x}O_4$ nanoparticles (a) x =0.0, (b) x =0.2, (c) x =0.4, (d) x =0.6, (e) x =0.8 and (f) x =1.0.

The obtained values of the lattice constant (*a*) are given in table 1. The lattice parameter is affected by several influencing factors such as the size of the atoms, interactive forces between the atoms, size of the final particle/grain [26] etc. It is found that the lattice parameters for the calcination temperature 600, 700 and 800℃ decreased from the un-substituted samples 8.370, 8.370, and 8.362 Å at (x=0) to 8.323, 8.350, and 8.360 Å respectively at (x=1.0) with increasing the Cr-substitution. The slight decrease in lattice constant may be due to slight difference in the ionic radii, larger size Fe^{3+} ions (ionic radius 0.645 Å) are being replaced by smaller Cr^{3+} ions (ionic radius 0.520Å).

The X-ray density values (ρ_x) are dependent on the molar mass of the synthesized compounds and the lattice parameter (*a*). For the calcination temperature at 600, 700 and 800℃ the values of (ρ_x) decreases linearly, it directly correlates with the decrease of molecular weight; however, it decreased with Cr^{3+} substitutions for all prepared samples as listed in table 1. This was attributed to the fact that atomic weight of the chromium is less than that of iron.

The distance between the magnetic ions, known as hopping length *L*, influences the physical properties of the ferrite system [27]. The calculated values of the hopping length L_A and L_B of different compositions were tabulated in Table 1. It can be observed that the tetrahedral and octahedral hoping length decreases with increase in mole percentage of chromium and increases as the temperature increase. The changes in the rate at which Cr^{3+} ions in the tetrahedral and octahedral sites with increase in Cr-substitution may be playing an important role in changing of the value of hopping length which is related to the fact that Cr^{3+} ion has smaller radius than Fe^{3+}ion [6].

Table 1. Values of crystallite size (*D*), Lattice parameter (*a*), X-ray density (ρ_x), hopping length (L_A) and (L_B) of $CoCr_xFe_{2-x}O_4$ nanoparticles.

X	***Concentration***	***Temp.***	***D(nm)***	***a(Å)***	***ρ_x(gm/cm^3)***	***L_A***	***L_B***
0.0	($CoFe_2O_4$)	as-burnt	38.791	8.361	5.332	3.6204	2.9561
		T=600℃	49.638	8.370	5.315	3.6241	2.9591
		T=700℃	54.161	8.370	5.315	3.6241	2.9591
		T=800℃	59.149	8.362	5.329	3.6210	2.9565
0.2	($Co\ Cr_{0.2}Fe_{1.8}O_4$)	as-burnt	15.451	8.357	5.322	3.6187	2.9547
		T=600℃	25.281	8.367	5.303	3.6229	2.9581
		T=700℃	43.456	8.369	5.299	3.6238	2.9588
		T=800℃	57.945	8.371	5.295	3.6247	2.9596
0.4	($Co\ Cr_{0.4}Fe_{1.6}O_4$)	as-burnt	------	------	------	------	------
		T=600℃	23.839	8.357	5.305	3.6186	2.9546
		T=700℃	41.511	8.367	5.286	3.6229	2.9581
		T=800℃	57.941	8.370	5.280	3.6243	2.9592
0.6	($CoCr_{0.6}\ Fe_{1.4}O_4$)	as-burnt	------	------	------	------	------
		T=600℃	27.820	8.335	5.329	3.6091	2.9468
		T=700℃	43.681	8.364	5.273	3.6218	2.9572
		T=800℃	51.497	8.369	5.265	3.6238	2.9588
0.8	($Co\ Cr_{0.8}Fe_{1.2}O_4$)	as-burnt	------	------	------	------	------
		T=600℃	26.084	8.326	5.328	3.6053	2.9437
		T=700℃	39.922	8.358	5.268	3.6190	2.9549
		T=800℃	50.873	8.362	5.259	3.6209	2.9565
1.0	($CoCrFeO_4$)	as-burnt	------	------	------	------	------
		T=600℃	23.187	8.323	5.316	3.6041	2.9428
		T=700℃	34.769	8.350	5.265	3.6157	2.9522
		T=800℃	46.352	8.360	5.245	3.6202	2.9559

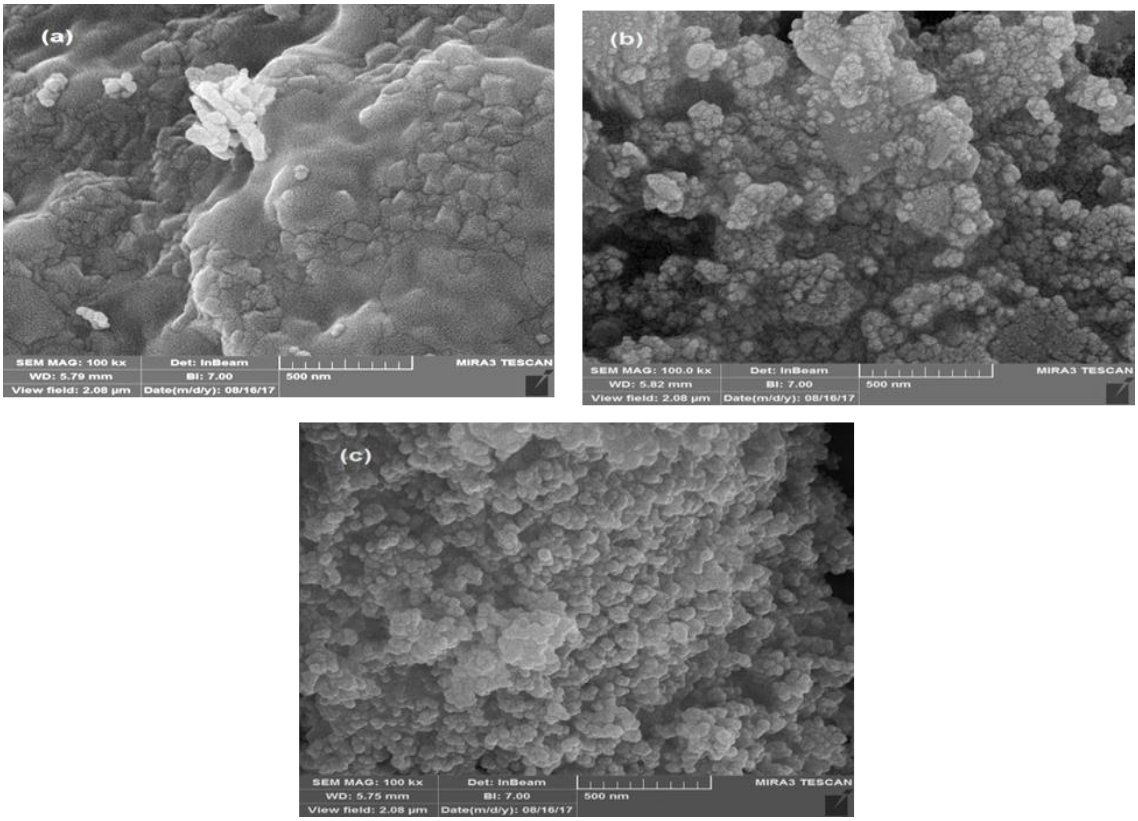

Figure 2. FE-SEM micrographs of $CoCr_xFe_{2-x}O_4$ nanoparticles calcined at 700 ˚C for; (a) x=0. (b) x=0.4 and (c) x=1.

FE-SEM study

The surface morphology and particle size of Cr-substitute cobalt ferrite nanoparticles $CoCr_xFe_{2-x}O_4$ (x = 0.0, 0.4, and 1.0) calcined at 700 ˚C have been investigated by FE-SEM image as shown in Fig. 2 (a–c).

It is evident that grain morphology, particle size, shape, uniformity, homogeneity and their distribution, are highly influenced by Cr^{3+} ions substitution and the average particle size goes on decreasing with increase in substitution of Cr^{3+} ions, suggesting that the presence of chromium inhibits crystal growth. It has been reported the substitution into a ferrite with strong site preferences ions, the particle size decreases with an increase in the substituted ion. This reduced is attributed to the flexibility of substitution into the available sites during particle growth, thus limiting the nucleation process and size [26]. The FE-SEM image of un-substituted cobalt ferrite (x = 0.0) as show in Fig. 2 (a) have the polyhedral shape with fine size, and relatively shows largest grains in an irregular and non-uniform manner compared with Fig. 2(b-c) that displayed a homogeneous microstructure and spherical shape with narrow particle size distribution. The porous structure formed might be due to the release of excess amount of gases during combustion method [28]. The appearance of some agglomerated areas in the FE-SEM images was due to the natural occurring interaction between magnetic nanoparticles and calcination temperature. In many cases of nanocrystalline spinel ferrites, it has been observed that there is a tendency for the nanoparticles to agglomerate [29].

Table 2. Average particle sizes of $CoCr_xFe_{2-x}O_4$ nanoparticles calcined at 700 ˚C with (x = 0.0, 0.4, and 1.0) determined from XRD and FE-SEM.

Cr content (x)	*Concentration*	*D(nm) XRD*	*D(nm) FE-SEM*
0.0	($CoFe_2O_4$)	54.182	68.434
0.4	($CoCr_{0.4}Fe_{1.6}O_4$)	41.511	53.827
1.0	($CoCrFeO_4$)	34.769	44.015

Table 2 demonstrates that the values of the estimated diameters of the $CoCr_xFe_{2-x}O_4$ nanoparticles with (x = 0.0, 0.4, and 1.0) that calcined at 700 ˚C with relatively well crystallized grains and an average particle size smaller than 68.434, 53.827, and 44.015 nm respectively, measured by Image J version 1.51j8 manufactured from National Institutes of Health Image Company, USA. All of these findings are in relatively good agreement with the XRD results. It is absorbed that the difference in the particle size for the present samples calculated by FE-SEM and the crystallite size obtained using Scherrer's formula from XRD analysis, may be due to the molecular structural disorder and lattice strain, which results from the different ionic radii and/or clustering of the nanoparticles. Hence, the XRD method has a more stringent criterion and leads to smaller sizes [30, 31].

Dielectric properties

The dielectric properties study for the ferrite nanoparticles supply us information about the electrical conduction mechanism in terms of the dielectric response in applied AC electric field. These properties are dependent on various factors such as preparation method, chemical composition, stoichiometry, porosity, ionic charge, grain size, and cation distribution between the tetrahedral and octahedral structures [10]. In the present study, the dielectric parameters such as Capacitance of the pellet, Dielectric loss angle (*tan δ*), and Capacitance of air with the same thickness as the pellet were measured using LCR meter at room temperature.

The real part of the dielectric constant (*ε′*), imaginary part of the dielectric constant (*ε″*) or dielectric loss factor, and the ac conductivity (σ_{ac}) were calculated using the following relations [32].

$$\varepsilon' = \frac{Cd}{\varepsilon_o A} \quad (6)$$

$$\varepsilon'' = \varepsilon' \tan\delta \quad (7)$$

$$\sigma_{ac} = 2\pi f \varepsilon_0 \varepsilon' \tan\delta \quad (8)$$

Where C is the capacitance of the pellet in farad, d is the thickness of the pellet in meter, A the cross-sectional area of the flat surface of the pellet, ε_o is the constant of permittivity of free space, and f is the frequency.

Fig. 3(a-d) shows a representative behavior of dielectric constant (*ε′*), dielectric loss angle (*tan δ*), dielectric loss factor (*ε″*), and ac conductivity (σ_{ac}) respectively as a function of frequency .

The stored energy is described by dielectric constant (*ε′*), It is clearly seen that the dielectric constant (*ε′*) is high in the range of low frequency and decreases with increasing frequency and finally reaches its minimum value at the high frequencies for all the samples, which indicates a normal behavior observed in most of the ferrite materials. Similar behavior was observed in our publications on Mg-Co Ferrites [33, 34]. This variation can be explained on the basis of that higher dielectric constant at lower frequency may be due to the simultaneous presence of different types of polarization contributions (space charge, dipolar, ionic, electronic, etc.) which is found to decrease with the increase in frequency [35]. The values of dielectric constant (*έ*) are calculated at difference frequencies (200 kHz, 500 kHz, and 1MHz) as shown in table 3. The decrease in dielectric constant with increasing frequency is due to the fact that at higher frequencies, any effect contributing to polarization is found to show lagging behind the applied field (the polarization contributions relax out) resulting in lowering of dielectric constant which is attributed to the contribution of electric polarizability only [36]. Also, the present investigation shown that the dielectric constant (ε') of Cr-substituted cobalt ferrite is higher than that of pure cobalt ferrite nanoparticles, which is good agreed with the earlier report [33]. The reason for these variations may be because of Cr concentration, which is reducing the hopping probabilities across the grain boundaries. This is increasing the charge accumulation at the grain boundaries and hence the dielectric constant value.

The dielectric loss represents the energy dissipation in a dielectric material and is defined in terms of dielectric loss angle (*tan δ*) and dielectric loss factor (*ε″*). It develops on account of lagging behavior of polarization from the applied ac field due to impurities and imperfections in the crystal lattice of the materials [37, 38]. Fig. 3 (b and c) shows the variation of dielectric loss angle and factor respectively as a function of frequency at room temperature and summarized in Table 3. It can be seen that the dielectric loss angle (*tan δ*) and dielectric loss factor (*ε″*) shows a decreasing trend with increase in frequency which is normal behavior of any ferrite materials and then it remains constant at high values. The decrease in the values of both (*tan δ*) and (*ε″*) with the frequency are elucidated with Maxwell–Wagner model [39]. and koop's theory [40]. In the high frequency region, which corresponds to a low resistivity (due to the grains), a small amount of energy is required for hoping of electrons between the two Fe ions (Fe^{2+} and Fe^{3+}) at the octahedral site while in the low frequency region, grain boundary are active due to high resistivity so large amount of energy is required for hoping of electron between two Fe ions at the B site. Thus one concludes that the possible mechanism for the dielectric behavior of the investigated ferrite samples is of two layers type [41].

The dielectric loss (*tan δ*) and (*ε″*) have a large values for the un-substituted cobalt ferrite (x=0) as well as these values decrease from (x=0.2–1.0) with increasing Cr-substitution. This shows that with increase in Cr-substitution, the energy losses decrease at high frequencies. This makes them possible materials for applications at high frequency. The incorporation of chromium in the place of iron has been successful in reducing the dielectric loss as it is observed in the Fig. 3 (a and b).

Interfacial regions like the surface of material, grain boundaries contain more defects or imperfections comparably to intrinsic grain region. The suppression of surface conduction due to Cr-substitution in cobalt ferrite may reduce the dielectric loss overall in the spectrum. This kind of observation was also noted by other researchers[1, 6], which indicates a very low loss in signal during its passage from the materials. The dielectric loss angle and factor also depends on different factors, such as stoichiometry, Fe^{2+} content, and structural homogeneity which in turn depend upon the composition and sintering temperature of the samples [33, 38].

The variation of ac conductivity (σ_{ac}) with respect to the applied frequency for a series of $CoCr_xFe_{2-x}O_4$ with x=0.0, 0.2, 0.4, 0.6, 0.8, and 1.0, at room temperature are represented in Fig. 3(d). The ac conductivity gradually increases as the frequency of applied field increases and slowly increases at higher frequencies. At lower frequencies the grain boundaries are more effective than grains in electrical conduction hence the hopping of Fe^{2+} and Fe^{3+} ions are bound at lower frequencies. It is evidence from the figure that ac conductivity becomes more and more frequency dependent. The frequency dependent ac electrical conductivity of ferrites is generally accepted due to electron hopping between Fe^{2+} and Fe^{3+} ions on the B sites [42].

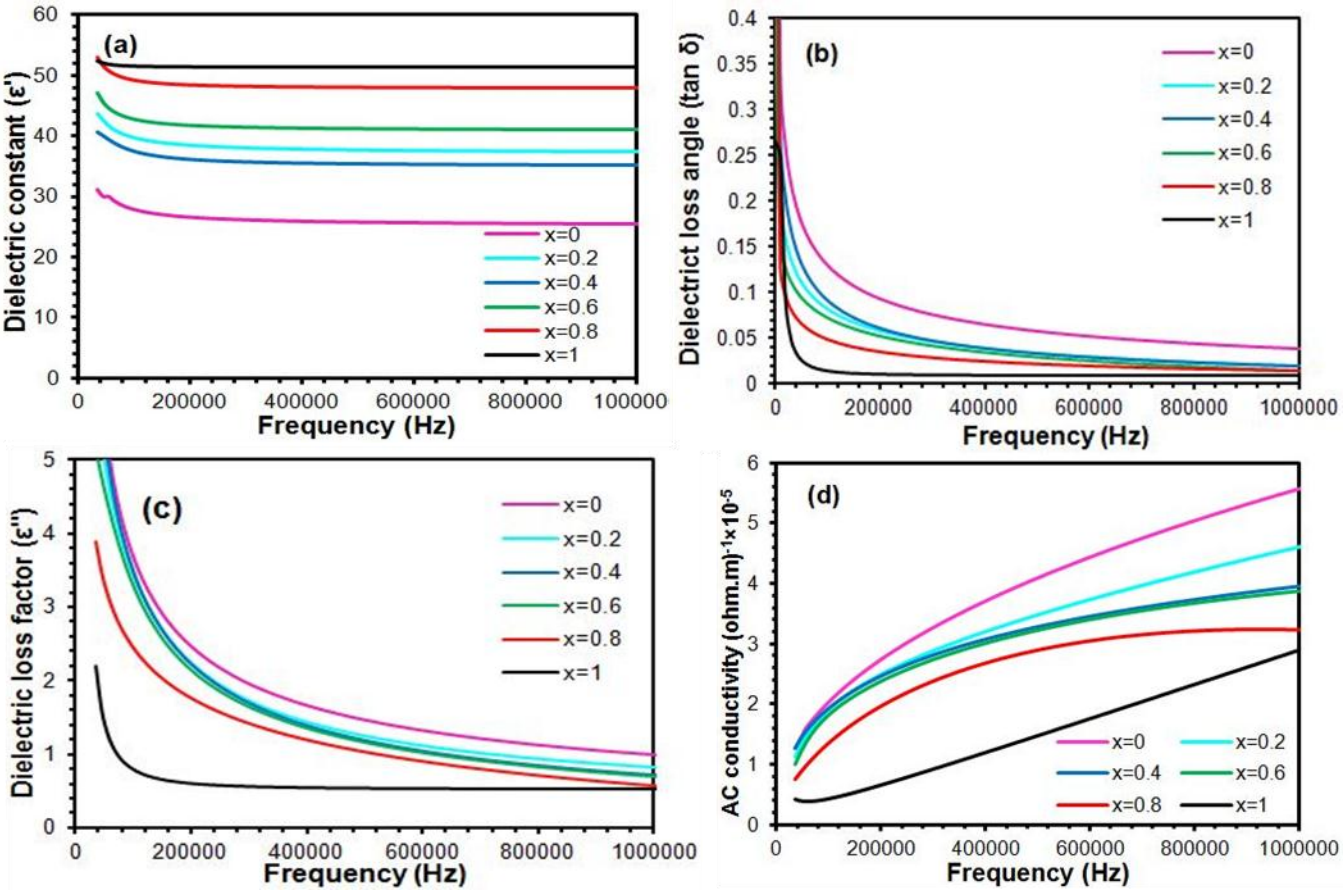

Figure 3. Dielectric properties of $CoCr_xFe_{2-x}O_4$ nanoparticles as a function of frequency, (a) dielectric constant (ε'), (b) dielectric loss angle ($tan\ \delta$), (c) dielectric loss factor (ε''), and (d) ac conductivity (σ_{ac}).

The frequency dependent variation of ac electrical conductivity has been explained on the basis of Maxwell–Wagner's double layer model for dielectrics. As a result, the grain boundaries at lower frequencies are more active. Hence at lower the frequency, the electron hopping frequency between $Fe^{2+} \leftrightarrow Fe^{3+}$ are very much hindered. Therefore, the observed conductivity of the materials at lower frequency is less. However, as the frequency of the applied field increases, the conductive grains are become more active by promoting the hopping between the Fe^{2+} and the Fe^{3+} ions on the octahedral sites, and thereby supporting to the hopping of electron between neighboring ions. As a result, the electrical conductivity increases gradually with increasing frequency [43, 44]**.** It is also clearly seen that the frequency dependent ac electrical conductivity are markedly dependent on the Cr-substitution in the cobalt ferrite nanoparticles materials. The highest and lowest value of conductivity were found at x=0 ($CoFe_2O_4$) and x=1 ($CoCrFeO_4$) respectively, which may be related to the partial substitution of Cr and the difference in the grain size. The conductivities of polycrystalline material decreases with decreasing grain size. Smaller grains imply large number of insulating grain boundaries and smaller grain-to-grain surface contact area, which act as a barrier to the flow of the electron and vice versa for increases the conductivity. Generally, the grain size, grain boundaries, porosity, crystal defects and stoichiometry are important factors influencing the conductivity and permittivity [25].

Table 4. Values of dielectric constant (ε'), dielectric loss angle ($tan\ \delta$), dielectric loss factor (ε'') and ac conductivity (σ_{ac}) at 200 KHz, 500 KHz and 1 MHz $CoCr_xFe_{2-x}O_4$ nanoparticles with (x=0.0 - 1.0) which calcined at 800℃ and sintered at 900℃

Cr content (x)	***0.0***	***0.2***	***0.4***	***0.6***	***0.8***	***1.0***
ε′ (200KHz)	26.60	38.50	36.10	41.80	48.40	51.40
tan δ (200KHz)	0.9300	0.0590	0.0615	0.0525	0.0345	0.0115
ε″ (200KHz)	2.46	2.24	2.20	2.14	1.76	0.60
σ^{ac} (200KHz)	2.75	2.49	2.46	2.38	1.97	0.66
ε′ (500KHz)	25.70	37.70	35.30	41.20	47.90	51.30
tan δ (500KHz)	0.0577	0.0345	0.0335	0.0295	0.0213	0.0105
ε″ (500KHz)	1.47	1.26	1.19	1.16	1.04	0.53
σ_{ac} (500KHz)	4.10	3.48	3.28	3.22	2.89	1.48
ε′ (1MHz)	25.40	37.40	35.10	41.00	47.80	51.20
tan δ (1MHz)	0.0385	0.0203	0.0197	0.0146	0.0136	0.0102
ε″ (1MHz)	1.00	0.83	0.71	0.69	0.58	0.52
σ_{ac} (1MHz)	4.10	3.48	3.28	3.22	2.89	1.48

CONCLUSIONS

A series of Cr-substituted cobalt ferrite nanoparticles with a chemical formula $CoCr_xFe_{2-x}O_4$ (x= 0.0, 0.2, 0.4, 0.6, 0.8 and

1.0) was synthesized by citrate-gel auto combustion method. The XRD pattern revealed that the crystalline phase appears after the thermal treatments at 600 ˚C with an additional peak have been observed. The calcined powders samples at 800 ˚C showed formation of spinel cubic structure with single phased for all Cr-substituted. The substitution of Cr^{3+} ions for Fe^{3+} ions in cobalt ferrite nanoparticles reduces the crystallite size and causes appreciable changes in the structural properties. FE-SEM image results show some agglomerated of spherical and polyhedral shape morphology with fine size. The dielectric properties have been examined as a function of frequency, and found a decree in dielectric constant with increasing frequency at room temperature, indicates the normal dielectric behavior for all the samples. The dielectric properties are strongly affected by the cation redistributions and the change in morphology associated with the increase in Cr-substitution. The dielectric constant (ε') was found to increase with an increase in Cr-substitution. Whereas the dielectric loss angle ($tan\ \delta$) and factor (ε'') and the conductivity (σ_{ac}) decrease with an increase in Cr-substitution. The low values of dielectric loss at higher frequencies show the potential applications in high-frequency applications. The behavior of dielectric constant and ac conductivity of all samples follows Koop's theory, Maxwell-Wagner polarization process, and hopping of electrons. It can be concluded that different changes occur in the structural and dielectric properties of Cr-substituted cobalt ferrite nanoparticles due to the rearrangements of trivalent metal cations at different sites

REFERENCES

[1] M. Raghasudha, D. Ravinder, and P. Veerasomaiah, "FTIR Studies and Dielectric Properties of Cr Substituted Cobalt Nano Ferrites Synthesized by Citrate-Gel Method," *Nanoscience and Nanotechnology,* vol. 3, no. 5, pp. 105-114, 2013.

[2] C. Ramana, Y. Kolekar, K. Kamala Bharathi, B. Sinha, and K. Ghosh, "Correlation between structural, magnetic, and dielectric properties of manganese substituted cobalt ferrite," *Journal of applied physics,* vol. 114, no. 18, pp. 183907, 2013.

[3] P. Hankare, U. Sankpal, R. Patil, I. Mulla, P. Lokhande, and N. Gajbhiye, "Synthesis and characterization of $CoCr_xFe_{2-x}O_4$ nanoparticles," *Journal of Alloys and Compounds,* vol. 485, no. 1-2, pp. 798-801, 2009.

[4] M. Sugimoto, "The past, present, and future of ferrites," *Journal of the American Ceramic Society,* vol. 82, no. 2, pp. 269-280, 1999.

[5] I. Šafařík, and M. Šafaříková, "Magnetic nanoparticles and biosciences," *nanostructured materials*, pp. 1-23: Springer, 2002.

[6] R. Panda, R. Muduli, G. Jayarao, D. Sanyal, and D. Behera, "Effect of Cr^{3+} substitution on electric and magnetic properties of cobalt ferrite nanoparticles," *Journal of Alloys and Compounds,* vol. 669, pp. 19-28, 2016.

[7] Y. Köseoğlu, M. I. O. Oleiwi, R. Yilgin, and A. N. Koçbay, "Effect of chromium addition on the structural, morphological and magnetic properties of nano-crystalline cobalt ferrite system," *Ceramics International,* vol. 38, no. 8, pp. 6671-6676, 2012.

[8] I. Gul, W. Ahmed, and A. Maqsood, "Electrical and magnetic characterization of nanocrystalline Ni–Zn ferrite synthesis by co-precipitation route," *Journal of Magnetism and Magnetic Materials,* vol. 320, no. 3-4, pp. 270-275, 2008.

[9] M. J. Iqbal, Z. Ahmad, T. Meydan, and Y. Melikhov, "Temperature and composition dependence of magnetic properties of cobalt–chromium co-substituted magnesium ferrite nanomaterials," *Journal of Magnetism and Magnetic Materials,* vol. 324, no. 23, pp. 3986-3990, 2012.

[10] M. Vadivel, R. R. Babu, K. Sethuraman, K. Ramamurthi, and M. Arivanandhan, "Synthesis, structural, dielectric, magnetic and optical properties of Cr substituted $CoFe_2O_4$ nanoparticles by co-precipitation method," *Journal of Magnetism and Magnetic Materials,* vol. 362, pp. 122-129, 2014.

[11] B. Toksha, S. E. Shirsath, M. Mane, S. Patange, S. Jadhav, and K. Jadhav, "Autocombustion High-Temperature Synthesis, Structural, and Magnetic Properties of $CoCr_xFe_{2-x}O_4$ ($0\leq x\leq 1.0$)," *The Journal of Physical Chemistry C,* vol. 115, no. 43, pp. 20905-20912, 2011.

[12] M. J. Iqbal, and M. R. Siddiquah, "Electrical and magnetic properties of chromium-substituted cobalt ferrite nanomaterials," *Journal of Alloys and Compounds,* vol. 453, no. 1-2, pp. 513-518, 2008.

[13] A. Košak, D. Makovec, A. Žnidaršič, and M. Drofenik, "Preparation of MnZn-ferrite with microemulsion technique," *Journal of the European Ceramic Society,* vol. 24, no. 6, pp. 959-962, 2004.

[14] A. Hassadee, T. Jutarosaga, and W. Onreabroy, "Effect of zinc substitution on structural and magnetic properties of cobalt ferrite," *Procedia Engineering,* vol. 32, pp. 597-602, 2012.

[15] X. Jiao, D. Chen, and Y. Hu, "Hydrothermal synthesis of nanocrystalline $M_xZn_{1-x}Fe_2O_4$ (M= Ni, Mn, Co; x= 0.40–0.60) powders," *Materials research bulletin,* vol. 37, no. 9, pp. 1583-1588, 2002.

[16] A. Sutka, and G. Mezinskis, "Sol-gel auto-combustion synthesis of spinel-type ferrite nanomaterials," *Frontiers of Materials Science,* vol. 6, no. 2, pp. 128-141, 2012.

[17] M. Srivastava, S. Chaubey, and A. K. Ojha, "Investigation on size dependent structural and magnetic behavior of nickel ferrite nanoparticles prepared by sol–gel and hydrothermal methods," *Materials Chemistry and Physics,* vol. 118, no. 1, pp. 174-180, 2009.

[18] M. Margabandhu, S. Sendhilnathan, S. Senthilkumar, and D. Gajalakshmi, "Investigation of Structural, Morphological, Magnetic Properties and Biomedical applications of Cu^{2+} Substituted Uncoated Cobalt Ferrite Nanoparticles," *Brazilian Archives of Biology and Technology,* vol. 59, no. SPE2, 2016.

[19] S. Sharma, N. D. Sharma, N. Choudhary, M. K. Verma, and D. Singh, "Chromium incorporated nanocrystalline cobalt ferrite synthesized by combustion method: Effect of fuel and temperature," *Ceramics International,* vol. 43, no. 16, pp. 13401-13410, 2017.

[20] M. G. Naseri, E. B. Saion, H. A. Ahangar, A. H. Shaari, and M. Hashim, "Simple synthesis and characterization of cobalt ferrite nanoparticles by a thermal treatment method," *Journal of Nanomaterials,* vol. 2010, pp. 75, 2010.

[21] M. Sangmanee, and S. Maensiri, "Nanostructures and magnetic properties of cobalt ferrite ($CoFe_2O_4$) fabricated by electrospinning," *Applied Physics A,* vol. 97, no. 1, pp. 167-177, 2009.

[22] D. S. Nikam, S. V. Jadhav, V. M. Khot, R. Bohara, C. K. Hong, S. S. Mali, and S. Pawar, "Cation distribution, structural, morphological and magnetic properties of $Co_{1-x}Zn_xFe_2O_4$ (x= 0–1) nanoparticles," *RSC Advances,* vol. 5, no. 3, pp. 2338-2345, 2015.

[23] P. Hankare, V. Vader, N. Patil, S. Jadhav, U. Sankpal, M. Kadam, B. Chougule, and N. Gajbhiye, "Synthesis, characterization and studies on magnetic and electrical properties of Mg ferrite with Cr substitution," *Materials Chemistry and Physics,* vol. 113, no. 1, pp. 233-238, 2009.

[24] A. Raghavender, D. Pajic, K. Zadro, T. Milekovic, P. V. Rao, K. Jadhav, and D. Ravinder, "Synthesis and magnetic properties of $NiFe_{2-x}Al_xO_4$ nanoparticles," *Journal of Magnetism and Magnetic Materials,* vol. 316, no. 1, pp. 1-7, 2007.

[25] M. George, S. S. Nair, K. Malini, P. Joy, and M. Anantharaman, "Finite size effects on the electrical properties of sol–gel synthesized $CoFe_2O_4$ powders: deviation from Maxwell–Wagner theory and evidence of surface polarization effects," *Journal of Physics D: Applied Physics,* vol. 40, no. 6, pp. 1593, 2007.

[26] S. U. Bhasker, and M. R. Reddy, "Effect of chromium substitution on structural, magnetic and electrical properties of magneto-ceramic cobalt ferrite nano-particles," *Journal of Sol-Gel Science and Technology,* vol. 73, no. 2, pp. 396-402, 2015.

[27] R. Sridhar, D. Ravinder, and K. V. Kumar, "Synthesis and characterization of copper substituted nickel nano-ferrites by citrate-gel technique," *Advances in Materials Physics and Chemistry,* vol. 2, no. 03, pp. 192, 2012.

[28] S. Gowreesan, and A. R. Kumar, "Effects of Mg^{2+} ion substitution on the structural and electric studies of spinel structure of $Co_{1-x}Mg_xFe_2O_4$," *Journal of Materials Science: Materials in Electronics,* vol. 28, no. 6, pp. 4553-4564, 2017.

[29] M. G. Naseri, E. B. Saion, H. A. Ahangar, and A. H. Shaari, "Fabrication, characterization, and magnetic properties of copper ferrite nanoparticles prepared by a simple, thermal-treatment method," *Materials Research Bulletin,* vol. 48, no. 4, pp. 1439-1446, 2013.

[30] C. Ragupathi, J. J. Vijaya, L. J. Kennedy, and M. Bououdina, "Combustion synthesis, structure, magnetic and optical properties of cobalt aluminate spinel nanocrystals," *Ceramics International,* vol. 40, no. 8, pp. 13067-13074, 2014.

[31] C. Sujatha, K. V. Reddy, K. S. Babu, A. R. Reddy, and K. Rao, "Effects of heat treatment conditions on the structural and magnetic properties of MgCuZn nano ferrite," *Ceramics International,* vol. 38, no. 7, pp. 5813-5820, 2012.

[32] E. Pervaiz, and I. Gul, "Enhancement of electrical properties due to Cr^{3+} substitution in Co-ferrite nanoparticles synthesized by two chemical techniques," *Journal of Magnetism and Magnetic Materials,* vol. 324, no. 22, pp. 3695-3703, 2012.

[33] V. Vinayak, P. P. Khirade, S. D. Birajdar, R. Alange, and K. Jadhav, "Electrical and dielectrical properties of low-temperature-synthesized nanocrystalline Mg^{2+}-substituted cobalt spinel ferrite," *Journal of Superconductivity and Novel Magnetism,* vol. 28, no. 11, pp. 3351-3356, 2015.

[34] N. Thomas, P. Jithin, V. Sudheesh, and V. Sebastian, "Magnetic and dielectric properties of magnesium substituted cobalt ferrite samples synthesized via one step calcination free solution combustion method," *Ceramics International,* vol. 43, no. 9, pp. 7305-7310, 2017.

[35] R. Ranjan, R. Kumar, and R. Choudhary, "Effect of Sm Substitution on Structural, Dielectric, and Transport Properties of PZT Ceramics," *Physics Research International,* vol. 2009, 2009.

[36] M. Lakshmi, K. V. Kumar, and K. Thyagarajan, "Study of the Dielectric Behaviour of Cr-Doped Zinc Nano Ferrites Synthesized by Sol-Gel Method," *Advances in Materials Physics and Chemistry,* vol. 6, no. 06, pp. 141, 2016.

[37] Y. Kolekar, L. Sanchez, and C. Ramana, "Dielectric relaxations and alternating current conductivity in manganese substituted cobalt ferrite," *Journal of Applied Physics,* vol. 115, no. 14, pp. 144106, 2014.

[38] R. Ahmad, I. H. Gul, M. Zarrar, H. Anwar, M. B. khan Niazi, and A. Khan, "Improved electrical properties of cadmium substituted cobalt ferrites nano-particles for microwave application," *Journal*

of Magnetism and Magnetic Materials, vol. 405, pp. 28-35, 2016.

[39] K. W. Wagner, "The Distribution of Relaxation Times in Typical Dielectrics," *Annals of Physics,* vol. 40, pp. 817-819, 1973.

[40] C. Koops, "On the dispersion of resistivity and dielectric constant of some semiconductors at audiofrequencies," *Physical Review,* vol. 83, no. 1, pp. 121, 1951.

[41] A. Sattar, and S. A. Rahman, "Dielectric properties of rare earth substituted Cu–Zn ferrites," *physica status solidi (a),* vol. 200, no. 2, pp. 415-422, 2003.

[42] R. S. Yadav, I. Kuřitka, J. Vilcakova, J. Havlica, J. Masilko, L. Kalina, J. Tkacz, J. Švec, V. Enev, and M. Hajdúchová, "Impact of grain size and structural changes on magnetic, dielectric, electrical, impedance and modulus spectroscopic characteristics of $CoFe_2O_4$ nanoparticles synthesized by honey mediated sol-gel combustion method," *Advances in Natural Sciences: Nanoscience and Nanotechnology,* vol. 8, no. 4, pp. 045002, 2017.

[43] M. T. Rahman, M. Vargas, and C. Ramana, "Structural characteristics, electrical conduction and dielectric properties of gadolinium substituted cobalt ferrite," *Journal of Alloys and Compounds,* vol. 617, pp. 547-562, 2014.

[44] K. Verma, A. Kumar, and D. Varshney, "Dielectric relaxation behavior of $A_xCo_{1-x}Fe_2O_4$ (A= Zn, Mg) mixed ferrites," *Journal of Alloys and Compounds,* vol. 526, pp. 91-97, 2012.